IOSR Journal of Mechanical and Civil Engineering (IOSR-JMCE)
e-ISSN: 2278-1684,p-ISSN: 2320-334X, Volume 14, Issue 1 Ver. VII (Jan. - Feb. 2017), PP 14-22
www.iosrjournals.org

"Hot Rotary Kiln Deformability for Cement Plant, Experimentation, and Numerical Simulation"

Khalid Idrissi Janati[1], Essaid El Kennassi[2], Lahbib Bousshine[3]
[1]*ENSEM, Hassan II University, BP 8118, Oasis, Casablanca, Morocco*
[2]*ENSEM, Hassan II University, BP 8118, Oasis, Casablanca, Morocco*
[3]*ENSEM, Hassan II University, BP 8118, Oasis, Casablanca, Morocco*

Abstract: *The goal of this work is the study of mechanical behavior and ferrule deformability under the heat effect, for a cement plant's rotary kiln. This study is within the scope of preventive maintenance for these kilns more specification precisely. It's about the finite element model validation, which simulates the kiln's elastoplastic behavior. This work is based on the case study of a cement plant's rotary kiln of a Moroccan industrial group. First, we take experimental measurements for the kiln distortions in the presence of heat. The, we use the numerical finite element method to simulate the ferrule and the refractory wall, this simulation is obtained by the use the of commercial software PATRAN-NASTRAN. Finally For a better reality approach of the kiln behavior, our finite element method results are compared with those obtained by the experimental tests.*

Keywords: *Deformability, Ferrules, Numerical Simulation, Ovality, Patran/Nastran, Preventive Maintenance, Refractory Bricks, Rotary Kiln.*

I. Introduction

In the scope of preventive maintenance (Levitt, 2003) a detailed study of the kiln (Figure 1) should be elaborated. To do this, it is necessary to determine the ovality of kiln (Montadher, 2012) sections so as to anticipate the falling of refractory bricks and to detect the real rotary axis to be able to counter the misalignment problem. These causes have a huge influence on other components of the kiln, for example, the guide rollers in the rotation which are in order of three as it is shown in the figure.

Figure 1. Rotary kiln

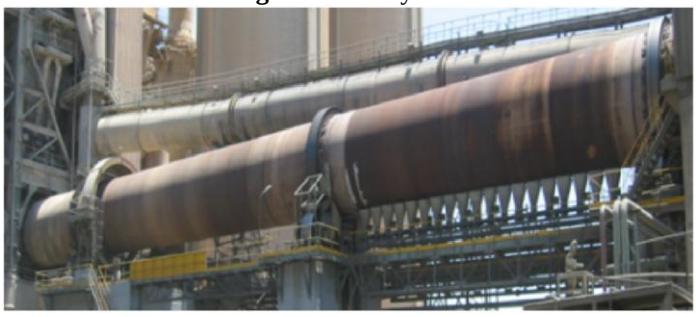

To protect the kiln ferrule, and other components and to and also avoid an excessive loss of heat. The rotary kiln is garnished with, refractory, a special coating, Figure 2. (Mujumdar, 2007) and (Boateng, 2008).

Figure 2. Firebricks inside the ferrule

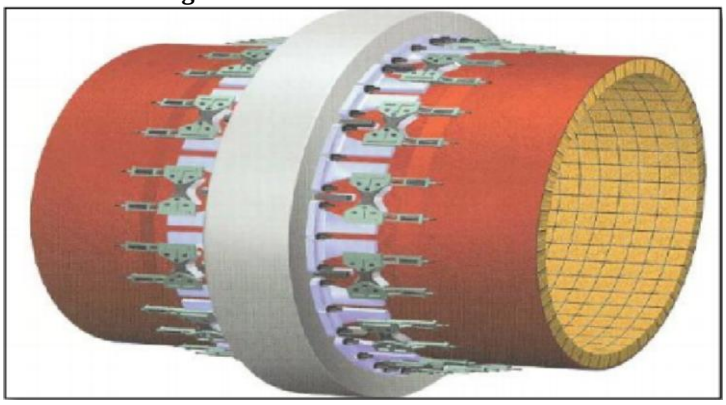

The ferrule consists of several sections. Arranged by welding and coated with refractory bricks (Ghanbarezhad, 2013) and (Ono, 2004). Each section has a specific thickness, so as to resist to applied stress (Mujumdar, 2007).

For the kiln, then expected thermal constraints define the steel grade. While in service, the kiln internal temperature in service differs as we go away to the entrance. So, it is necessary to control permanently the outside heat of the ferrule by suitable measurement apparatus. Moreover, it is recommended to make a visual control once a day. The reference value of the maximum temperature of the ferrule is 350°C. In our case, the used steel for kiln ferrules does not have a resistance to temperatures above 350°C.

During kiln service, at the ferrule level, the temperature may sometimes exceed the accepted value. The main cause lies in a damaged bricklaying or a thin bracketing layer as a result of wear (Shijie, 2006). The replacement of the brick coating in the observed heat zones of the ferrule is of a great priority. Furthermore, temperature differences of the kiln circumference provoked by a unilateral crusting or red spot caused deformations of the ferrule, all lead to temporary curves of the cylinder (Ghoshdastidar, 2002).

This has a result on the rotary kiln ferrule constrains, which. According to the curve degree, may grow up to n-times the admissible stress. These excessive constraints may lead to the creation of cracks in the metal sheet of the ferrule.

In addition, all the rolling positions, (bandages, roll, ferrules) are subject to more important stress. The kiln deformation engenders an eccentricity in the ring gear and in the pinion. In the case of extreme curves which occur while the kiln is cold, measures should be taken to restore the kiln according to its longitudinal axis. These measures must be realized by a highly specialized staff (Mujumdar, 2006).

II. Geometry

The rotary kiln is a long cylinder inclined in continuous rotation for the movement of the material. a burner heats the material, and the hot gases circulating in the opposite direction of media movement. the shell of the rotary kiln is composed of several different sizes of sections welded together and coated with refractory bricks. Each section of the kiln has a specific thickness and materials are chosen to withstand the stresses applied to the mechanical and thermal loads Kilns range in size from 2–6 m in diameter and can be 50–225 m long with an operating mass of up to 3000 t.

The rotary kiln has a strip-rolled sheet per support known as a tyre. Each one is dimension edwith the same inner and outer diameters as well as the same contact length on the support rollers. Each tyre is situated on a roller station and each roller station is supported on a concrete foundation. In this model, rollers are situated forming a triangle with the center of the clinker kiln body as shown in Fig 3.

The installation components are as follows:

- Rotary kiln shell.
- Kiln tyres.
- Tyre-bearing kiln shell sections.
- Roller stations.
- Drive components(not shown here).
- Toothed ring and drive pinion (not shown here)

Figure 3. Simple scheme of the kiln

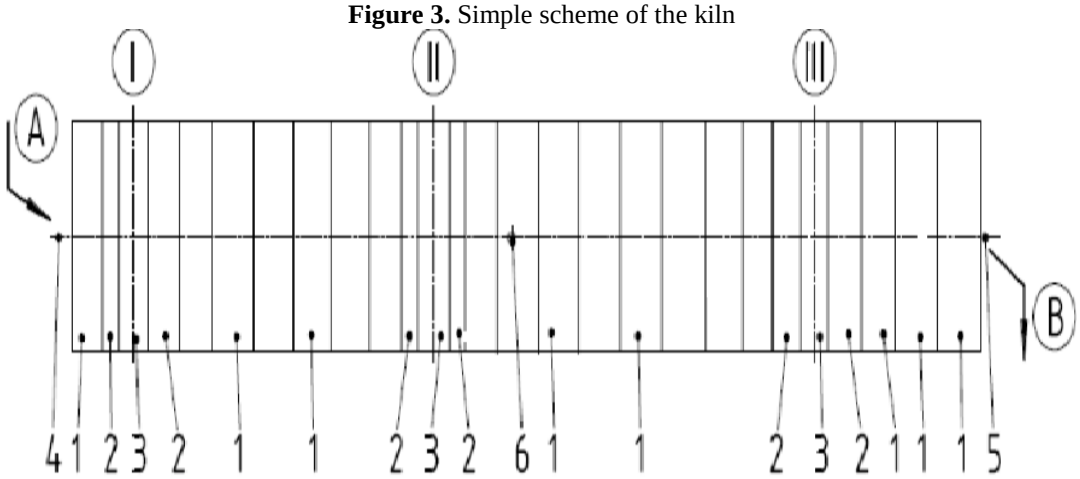

The inclination and the displacement of limestone in the entrance of kiln (A) through the ferrule towards the exit of the latter (B) in the form of a link as shown in Figure 3.

Ferrules main material

The kiln ferrules are made by an ordinary E24 metal (Lemaitre, 2004) assembled by a weld bead made of a second material (ASME, code II, and VIII). To simplify the calculations, we suppose that the entire ferrule material is in E24 metal which characteristics are given in the following Table 1.

Table 1: Mechanical characteristics of steel E24

Material properties	Values
Young's modulus	210000MPa
Poisson coefficient	0.3
elastic limit	235MPa
Breaking load	40DaN/mm²

Refractory bricks materials

The refractory bricks [4] of the kiln which are made of composite material, larked to each other in a special form, so as to facilitate the adherence to the ferrule Figure 3, the material characteristics are given in the following Table 2.

Table 2: Mechanical characteristics of the

Material properties	Values
Young's modulus	105000MPa
Poisson coefficient	0.35
elastic limit	90MPa
Breaking load	120N/mm²

Measurement method

Special apparatus for measuring is used, a personal computer (PC) for data acquisition and a tripod as a support. In order to measure, it is necessary to stay next to the kiln. Hence we define two types of coordinates. A global one (upstream joint as a landmark) the role of this coordinate system is determining the position of the station in relation to the center of the ring. And a local one.

Figure 4. The deformability measuring apparatus

III. Determining The Ovalization

To determine the ferrule ovalization (Mujumdar,2006). As shown in Figure 5 we need to identify the position of the station with a global landmark. By inserting the angle of the station deviation, we deduce the distance that separates a given measurement point to the center, the center is determined to be between the kiln wheels. Practically, ovality can be measured with a simple device shown in Fig.4.It consists of a pointer and a recording plate. The pointer is attached to the kiln shell by a magnet and pressed in contact with the recording plate which is secured with help of a magnet on to the tire. The creep "U" and the tire clearance "S" can be read directly from the plotted profile. Or the creep can be determined by suitably marking tire and the shell and then by measuring displacement between tire and shell.

The technique for Rotary Kiln ovality measurement, by Shell test apparatus, has been developed way back in the beginning of 1950's by G. Rosenblad[6].Theoretically ovality will be simulated numerically in order to make comparison with practical side using software (Patran/Nastran) based on Finite Element Method.

The temperatures distribution of the kiln shellwas measured practically by simple device called kiln shell scanner (Field located analyzer that measures the temperature of a kiln shell.), this device connected to computers in the control room using special software.

Figure 5. A section ovalization on the ferrule

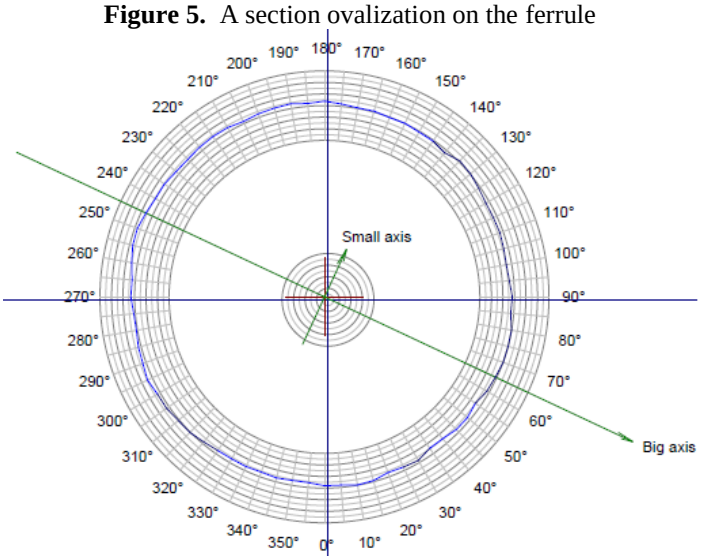

Numerical simulation using the finite element method

The objective of this study is to analyse the plastic behavior of kiln ferrule, in the case of static loads. Firstly, a numerical task was (Zienkiewicz, 2005) and (Ventsel, 2001). conducted to take a decision on the preventive maintenance of the kiln. All simulations were done by the method of calculation by finite elements Patran/Nastran (Janati, 2015) and (Biron, 2011)

The model structure consists of two parts.

- Definition of the simplified model.
- Definition of the type of the calculation model including different modules which enable to write.
  - The geometries.
  - The used material.
  - The boundaries and loading conditions types of unstructured grid.

We have a kiln with a big dimension (Kohar, 1995), so in order to see the limits conditions, the loading and the grid structure in the model, we have enlarge the zones shown in Figure 6.

Figure 6. The kiln with boundary conditions, grid structure and loading

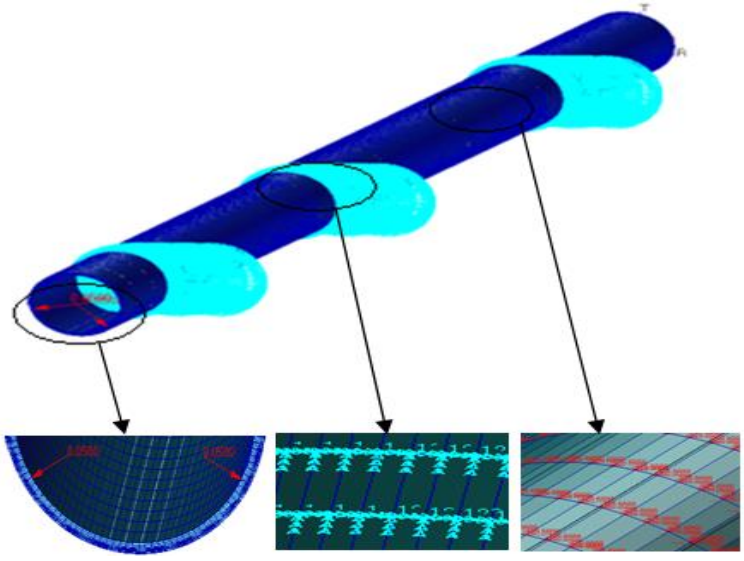

Numerical and experimental ovalization

To measure the ovalizations, we take some sections of the kiln ferrule, and then we determine the maximal movement on each ferrule section. By choosing some landmarks of sections with experimental measures ovalizations, we validate the numerical results in relation with those obtained by experimentation. For this reason we have chosen a single section on the upstream kiln. Figure 7 shows the numerical ovalization by Patran/Nastran upstream kiln.

Figure 7. Upstream ovalization

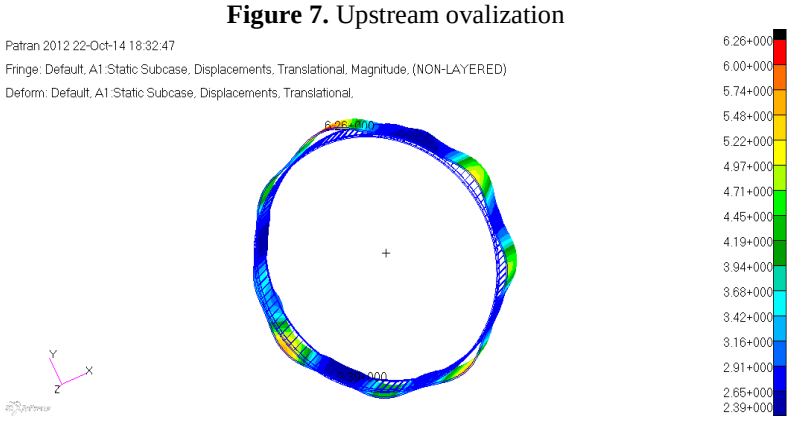

We conclude by the Table 3, the maximal values of the two numerical and experimental methods. We found very close values, as shown in Table 3.

Table 3. Eccentricity values

Abscissa 0 (Upstream)	Eccentricity (mm)
Numerical	8.65
Experimental	8

IV. Experimental and numerical kiln displacements

We divide the kiln into three upstream parts, the middle parts is downstream (Pisaroni, 2012). To conduct a comparative study of the first four meters of the kiln. In Figure 8, the curve appears in two lines so, we have noticed a slight difference between the two curves. For the second zone, it appears a difference between the two curves which is due to the ferrule's fatigue.

Figure 8. Displacement of the kiln upstream

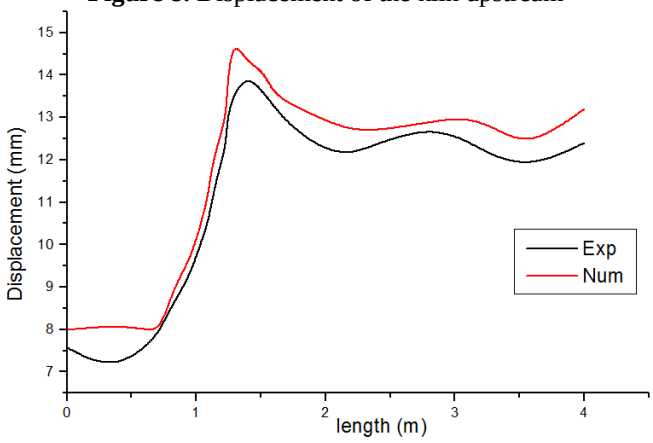

Figure 9. Displacement in the middle kiln

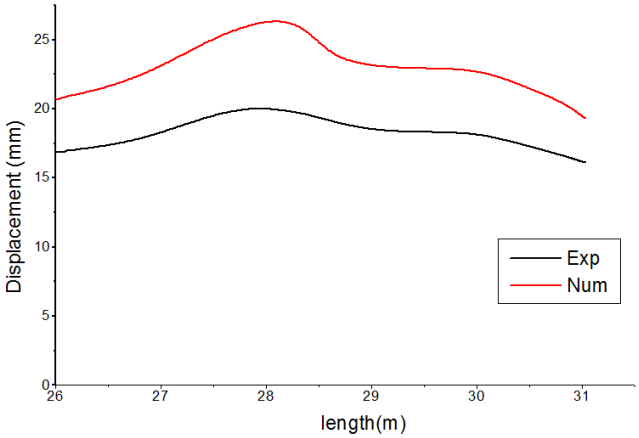

Figure 10. Displacement of the kiln downstream

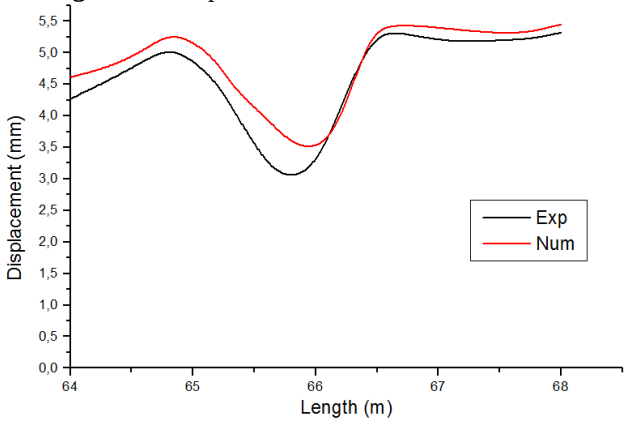

A Comparison between solid and shell mesh

In this paragraph, we try to study kiln. We mesh the kiln ferrule by two types of elements. We consider the solid elements in the first case and the shell elements in the second case for the same kiln (Del Coz Diaz, 2002). The objective of this study is to show the difference between the two types of meshing. In the second case, we use a shell mesh for the outside ferrule. The contact between the refractory bricks and the ferrule is defined as an adherence contact.

Figure 11. Solid and shell mesh of kiln

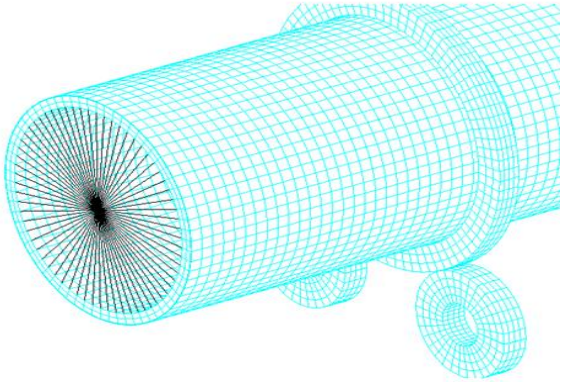

Upstream deformability of the kiln

We mark the movement in an upstream section of the kiln (the entry) for both types of meshing. The results are represented in Figure 12. We notice a difference between the two curves in the 90° angle in relation to the horizontal axis, which is the angle of the transported loadings (Pazand, 2009).

Figure 12. The round function movement of the kiln

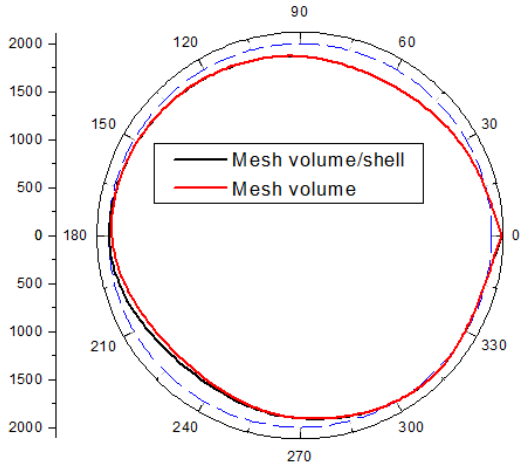

Section (°)

Band deformability

We mark the movement in a section of the nearest zone to the first downstream band of the kiln for both types of meshing. The results are represented in Figure 13. We notice a difference between the two curves in the 90° angle in relation to the horizontal axis which is the angle of concentration of the transported loading.

Figure 13. Angle function movement of the kiln

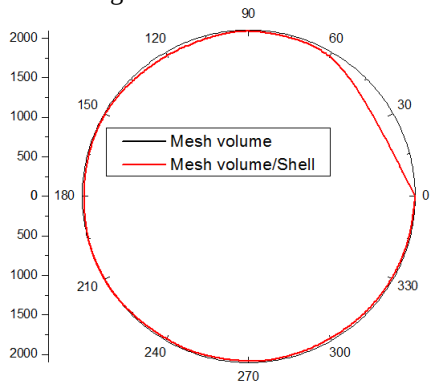

Section (°)

The results in the middle of the kiln

The graph below, Figure 14, shows the difference between the obtained results of both types of meshing in the middle of a kiln section.

Figure 14. Angle function displacement of kiln

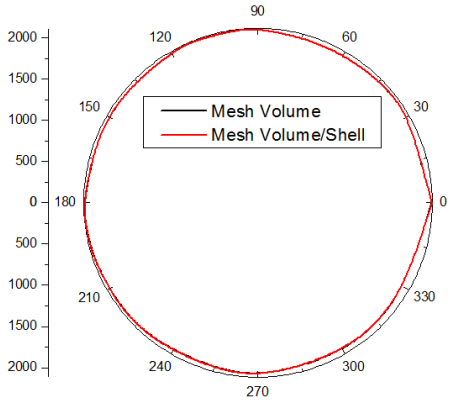

Section (°)

Comparison between two types of meshing in different kiln section

The graph presented in Figure 15, shows the difference between the maximum movements in terms of kiln height, obtained by the two types of meshing.

Figure 15. Displacements along the kiln

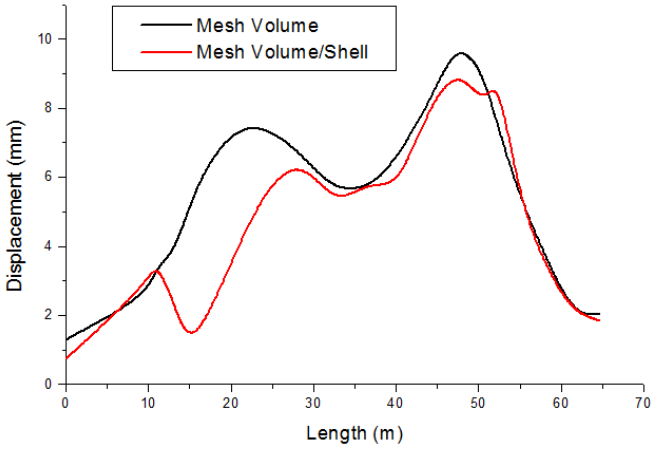

Kiln thermal deformations representation (ovalization)

The comparison was elaborated between two different approaches. The first approach, which is based on an experimental measurement campaign (Sonavane, 2009) and (Barr, 1989), this campaign is taken when the heat kiln is in rotation. The second approach is based on the numeric simulation which uses the same experimental load conditions. Figure 16 presents numeric and experimental displacements evolution, which is function of kiln length.

Figure 16. Comparison between heat measurements and thermo-mechanical calculus

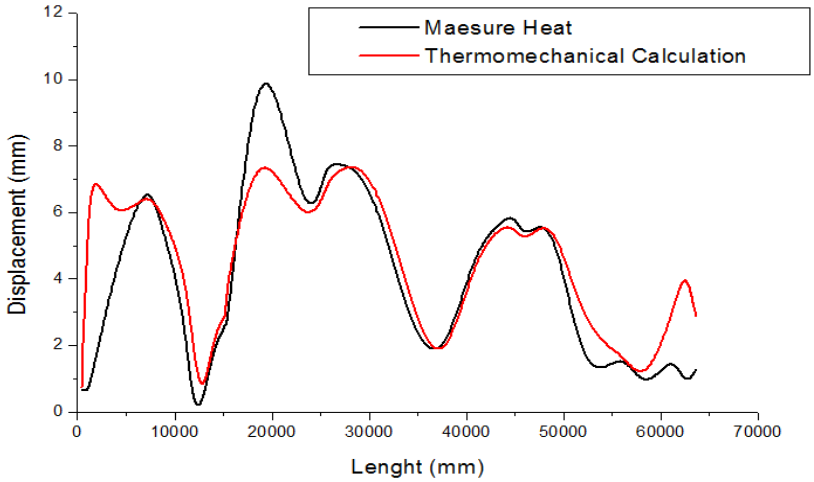

Kiln deformability experimental measurements and numeric calculus comparison

Figure 17 presents displacements values function of kiln length, which are obtained by the two approaches experimental and numeric (Ghoshdastidar, 2002) and (Boateng, 1995). We can show that the resulted curves present a sinusoidal evolution. This is due to the system support used.

Figure 17. Comparison between cold measurements with thermo-mechanical calculus, and the calculus obtained from thermal and mechanical loads

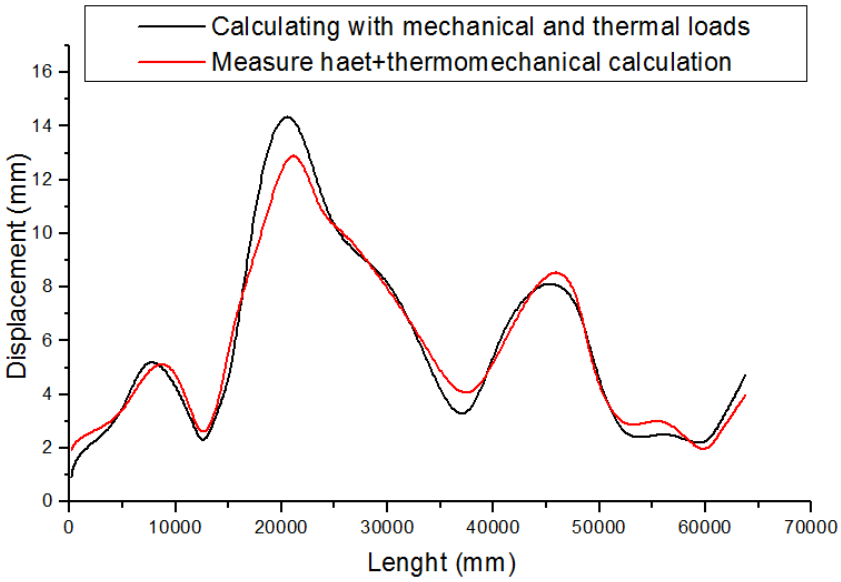

V. Conclusion

A comparative study between the experimental results and those obtained by the numerical simulation upon three critical zones of the rotary cement kiln is done. We notice that the three diagrams are close to each other as shown in Figure 13 to Figure 17. The next step that we would conduct is a thermal calculation on MARC, special thermal software. The main objective is to determine the complete deformability by measures, and thermal deformations through numerical calculation. Based on these values, we would obtain the mechanical deformation of the ferrule in which lodes are applied.

References

[1]. Asme Boiler and Pressure Vessel Code II. (1995). Material properties, *The American Society of Mechanical Engineers.*

[2]. Asme Boiler and Pressure Vessel Code VIII. (1995). Division 2 – Alternative rules, *The American Society of Mechanical Engineers.*

[3]. Barr, P. V., Brimacombe, J. K., & Watkinson, A. P., (1989). A heat-transfer model for the rotary kiln : Part II. Development of the cross-section model. *Metallurgical Transactions B,* Vol. 20B, 403-419.

[4]. Biron, A., & Hodge, P. G. (2011). Limit analysis of rotationally symmetric shells under central loadings by a numerical method. *Journal of Applied Mechanics,* 34(3), 644-650.

[5]. Boateng, A. A., & Barr, P. V., (1995). A thermal model for the rotary kiln including heat transfer within the bed. *Int. J. Heat Mass Transfer. Elsevier Science Ltd.* Vol. 39, No. 10, 2131-2147.

[6]. Boateng, A. A., (2008). Rotary kilns transport phenomena and transport processes. Oxford, *Butterworth – Heinemann, Elsevier.*

[7]. Del Coz Diaz, J. J., Rodriguez Mazon, F., Garcia Nieto, P. J., & Suarez Dominguez, F. J., (2002). Design and finite element analysis of a wet cycle cement rotary kiln. *Finite Elements in Analysis and Design,* 39, 17-42.

[8]. Ghanbarezhad, S., Nemati, A., Bavand-Vandchali, M., & Naghizadeh, R. (January, 2013). New development of spinel bounded chrome-free basic brick. *Journal of Chemical Engeneering Materials Science,* Vol. 4(1), 7-12.

[9]. Ghoshdastidar, P. S., Bhargava, G., & Chhabra, R. P., (2002). Computer simulator of heat transfer during drying and preheating of wet iron ore in a rotary kiln. *Marcel Dekker, Inc.*

[10]. Janati, K., Mjidila, A., Jalal, SE., & Bousshine, L. (2015). Limit analysis of a S235- steel bottle for calor gas for domestic usage. *IOSR Journal of Mechanical and Civil Engineering,* Vol. 12, Issue 2, Ver. II, 16-22.

[11]. Kohar, T., Richardson, J. T., & Dan Luss, (1995). Axial dispersion of solid particles in a continious rotary kiln. *AICHE Journal,* Vol. 41, No. 11.

[12]. Lemaitre, J., & Chaboche, J-L. (2004). Mécanique des matériaux solides. Paris, *Dunod.* Codap. (2010). Code de construction des appareils à pression non soumis à l'action de la flamme. *SNCT.*

[13]. Levitt, J., (1952). Complete guide to preventive and predictive maintenance, (second edition). New York. *Industrial Press Inc*.

[14]. Montadher, A. M., (2012). The ovality problem in cement kilns: A numerical and experimental study. *The Iraqi Journal for Mechanical and Material Engineering,* Vol. 12, No. 2, 239-266.

[15]. Mujumdar, K. S., & Ranade, V. V., (2007). CFD modeling of rotary cement kilns. *Asia-Pac. J. Chem.,* Vol. 3, 106-118.

[16]. Mujumdar, K. S., Arora, A., & Ranade, V. V., (2006). Modeling of rotary cement kilns: applications to reduction in energy consumption. *Ind. Eng. Chem. Res.* 45, 2315-2330.

[17]. Mujumdar, K. S., Ganesh, K. V., Kulkarni, S. B., Ranade, V. V., (2007). Rotary cement kiln simulator (RoCKS): Integrated modeling of pre-heater, calciner, kiln and clinker cooler. *Chemical Engineering Science, Elsevier,* Vol. 62, 2590-2607.

[18]. Mujumdar, K. S., Ranade, V. V., (2006). Simulation of rotary cement kilns using a one-dimensional model. *Chemical Engineering Research and Design,* 84(A3), 165-177.

[19]. Ono, M., & Kozuka, H., (May, 2004). Damage of refractory bricks lined in cement rotary kiln. *Tehran International Conference on Refractories,* 515-524.

[20]. Pazand, K., Shariat Panahi, M., & Pourabdoli, M. (2009). Simulating the mechanical behavior of rotary cement kiln using artificial neural networks. *Materials and Design,* 30, 3468-3473.

[21]. Pisaroni, M., Sadi, R., & Lahaye, D., (2012). Counteracting ring formation in rotary kilns. *Journal of Mathematics in Industry. Springer Open Journal,* 1-19.

[22]. Shijie, W., Jidong, L., Weijie, L., & Zhijuan, H., (2006). Modeling of pulverized coal combustion incement rotary kiln. *Energy & Fuels,* Vol. 20, 2350-2356.

[23]. Sonavane, Y., & Specht, E., (2009). Numerical analysis of the heat transfer in the wall of rotary kiln using finite element method ANSYS. *Seventh International Conference on CFD in the Minerals and Process Industries, CSIRO,* Melbourne, Australia, 9-11.

[24]. Ventsel, E., & Krauthammer, T., (2001). Thin plates and shells: Theory, analysis and applications. New York, *Marcel Dekker, Inc.*

[25]. Zienkiewicz, O. C., & Taylor, R. L., (2005). The finite element method: its basis and fundamentals, Oxford, *Elsevier.*